Immunobiology xxx (2016) xxx–xxx

Contents lists available at ScienceDirect

Immunobiology

journal homepage: www.elsevier.com/locate/imbio

The impact of surface chemistry modification on macrophage polarisation

Hassan M. Rostam[a], Sonali Singh[a], Fabian Salazar[a], Peter Magennis[b], Andrew Hook[b], Taranjit Singh[b], Nihal E. Vrana[c,d], Morgan R. Alexander[b], Amir M. Ghaemmaghami[a,*]

[a] Immunology and Tissue Modelling Group, Division of Immunology, School of Life Science, University of Nottingham, Faculty of Medicine & Health Sciences, Queen's Medical Centre, Nottingham, NG7 2UH, UK
[b] Interface and Surface Analysis Centre, School of Pharmacy, University of Nottingham, UK
[c] Protip Medical, 8 Place de l'Hôpital, 67000 Strasbourg, France
[d] INSERM UMR 1121, 11 rue Humann, 67085 Strasbourg, France

ARTICLE INFO

Article history:
Received 8 February 2016
Received in revised form 1 June 2016
Accepted 10 June 2016
Available online xxx

Keywords:
Macrophage
Monocyte
M1
M2
Macrophage polarisation
Biomaterials
Surface chemistry
Oxygen plasma etching
Water contact angle
Foreign body response

ABSTRACT

Macrophages are innate immune cells that have a central role in combating infection and maintaining tissue homeostasis. They exhibit remarkable plasticity in response to environmental cues. At either end of a broad activation spectrum are pro-inflammatory (M1) and anti-inflammatory (M2) macrophages with distinct functional and phenotypical characteristics. Macrophages also play a crucial role in orchestrating immune responses to biomaterials used in the fabrication of implantable devices and drug delivery systems. To assess the impact of different surface chemistries on macrophage polarisation, human monocytes were cultured for 6 days on untreated hydrophobic polystyrene (PS) and hydrophilic O_2 plasma-etched polystyrene (O_2-PS40) surfaces. Our data clearly show that monocytes cultured on the hydrophilic O_2-PS40 surface are polarised towards an M1-like phenotype, as evidenced by significantly higher expression of the pro-inflammatory transcription factors STAT1 and IRF5. By comparison, monocytes cultured on the hydrophobic PS surface exhibited an M2-like phenotype with high expression of mannose receptor (MR) and production of the anti-inflammatory cytokines IL-10 and CCL18. While the molecular basis of such different patterns of cell differentiation is yet to be fully elucidated, we hypothesise that it is due to the adsorption of different biomolecules on these surface chemistries. Indeed our surface characterisation data show quantitative and qualitative differences between the protein layers on the O_2-PS40 surface compared to PS surface which could be responsible for the observed differential macrophage polarisation on each surface.

1. Introduction

Implanted biomaterials typically trigger an inflammatory immune response orchestrated by macrophages (Higgins et al., 2009). Often this results in a cascade of inflammatory and fibrotic events known as the foreign body response (FBR) (Bartoli and Godleski, 2010). FBR begins with protein adsorption on the implant surface, which promotes the adhesion of monocytes and macrophages (Shen et al., 2004). Macrophages are sensitive to microenvironmental changes and mount a rapid response to implanted materials. They can also fuse under the influence of the cytokines interleukin 4 (IL-4) and IL-13, forming foreign body giant cells (FBGCs). Macrophages and FBGCs induce infiltration and stimulation of immune cells (e.g. lymphocytes) and stromal cells (e.g. fibroblasts), leading to inflammation and fibrosis at the implant site (Rostam et al., 2015). FBR can end with sequestration of the implant within a fibrous capsule (Anderson et al., 2008). This creates mechanical and functional problems, and for devices such as electrodes, can mean the end of their functional life (Morais et al., 2010).

Macrophages are extremely plastic cells, adopting a wide spectrum of phenotypes in response to different stimuli (Sica and Mantovani, 2012). The physical, chemical, and topographical characteristics of implanted materials can affect macrophage polarisation, resulting in macrophages that are either predominantly pro-inflammatory or anti-inflammatory (Rostam et al., 2015).

Abbreviations: O_2-PS, oxygen plasma etched polystyrene; PS, polystyrene; RGD, arginine-glycine-aspartate; TCP, tissue culture plastic; WCA, water contact angle.

* Corresponding author.
E-mail address: amir.ghaemmaghami@nottingham.ac.uk (A.M. Ghaemmaghami).

http://dx.doi.org/10.1016/j.imbio.2016.06.010

Table 1
Forward and reverse primer sequences used for qRT-PCR.

Genes	Primers/probe	Sequence (5′–3′)
GAPDH	Forward	GAGTCAACGGATTTGGTCGT
	Reverse	GACAAGCTTCCCGTTCTCAG
STAT1	Forward	GGAAGGGGCCATCACATTCA
	Reverse	GTAGGGTTCAACCGCATGGA
SOCS1	Forward	CCCTGGTTGTTGTAGCAGCTT
	Reverse	TTGTGCAAAGATACTGGGTATATGT
IRF5	Forward	GCCATGAGCAGGGAAAGAAC
	Reverse	CCCTTAGGCAATTCCTCCTATACA
SOCS3	Life Technologies Hs02330328_s1 *(Taqman)*	
IRF4	Life Technologies Hs01056533_m1 *(Taqman)*	

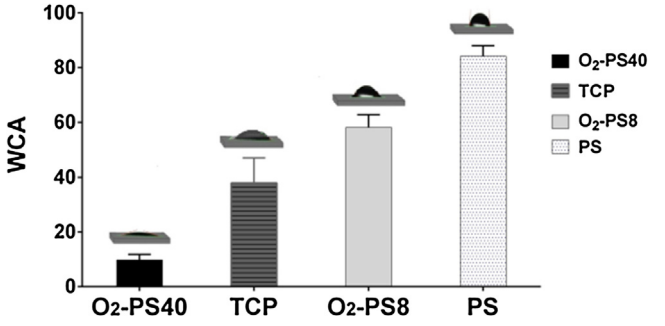

Fig. 1. Water contact angle (WCA) of polystyrene and TCP surfaces. The graph depicts the mean WCA ± SD for n = 4 oxygen plasma-etched polystyrene (O_2-PS40 and O_2-PS8), tissue culture plastic (TCP), and untreated polystyrene (PS) surfaces in ascending order of WCA.

The two best studied macrophage phenotypes are M1 and M2. M1 (classically activated) macrophages with pro-inflammatory and anti-tumour function (Sutterwala et al., 1997) can be generated *in vitro* from monocytes by treatment with the T helper (TH) 1 cytokine interferon gamma (IFN-γ) (Garcia et al., 2014) and/or lipopolysaccharide (LPS)(Mills et al., 2000). The addition of granulocyte macrophage colony-stimulating factor (GM-CSF) during M1 polarisation augments the pro-inflammatory function of these cells (Hamilton, 2002; Hamilton, 2008). By contrast, M2 (alternatively activated) macrophages with anti-inflammatory and pro-wound healing activities (Sutterwala et al., 1997) can be generated *in vitro* from monocytes by treatment with the TH2 cytokines IL-4 (Garcia et al., 2014; Verreck et al., 2004) and/or IL-13 (Garcia et al., 2014). The addition of macrophage colony-stimulating factor (M-CSF) during M2 polarisation can enhance the anti-inflammatory function of M2 macrophages (Garcia et al., 2014; Verreck et al., 2004).

M1 macrophages produce high levels of pro-inflammatory cytokines such as IL-12, IL-23 (Mantovani et al., 2004), tumour necrosis factor alpha (TNF-α) (Hofkens et al., 2011; Hao et al., 2012), IL-6, and IL-1β (Hofkens et al., 2011). They are also characterised by elevated expression of the chemokine (C-C motif) receptor 7 (CCR7)(Agrawal, 2012), CCR2 (Willenborg et al., 2012), calprotectin (Bartneck et al., 2010), and nitric oxide synthase 2, inducible (NOS2) (Edin et al., 2012). In contrast, M2 macrophages secrete large amounts of anti-inflammatory and pro-fibrotic cytokines such as IL-10 (Mantovani, 2006), transforming growth factor (TGF-β) (Hao et al., 2012), and IL-1 receptor antagonist (IL-1RA) (Baitsch et al., 2011). In addition, these cells express high levels of mannose receptor (MR) (Agrawal, 2012; Mantovani, 2006; Choi et al., 2010) and the scavenger receptor CD163 (Edin et al., 2012; Mantovani, 2006).

Additionally, M1 macrophages express high levels of prostaglandin-endoperoxide synthase 2 (Ptgs2 or Cox2) and IL23p19 genes, and exhibit phosphorylation of signal transducer and activator of transcription 1 (STAT1). M2 macrophages can be identified by high levels of Kruppel-like factor 4 (Klf4) and chitinase 3-like 2 (Chi3l2 or Ykl39) gene expression, and STAT6 phosphorylation (Murray and Wynn, 2011).

Appropriate regulation of macrophage activation post-implantation is extremely important, since these cells play a crucial role in the elimination of microbes and debris, biodegradation, tissue regeneration and vascularisation, and extracellular matrix reorganisation following tissue damage (Xia and Triffitt, 2006). Therefore, macrophages and FBGCs, either directly or through modulating the function of other cell types, can tip the balance between chronic inflammation and resolution/wound healing following biomaterial implantation (Solheim et al., 2000).

In order to minimise implant-associated inflammation, various approaches have been used to modulate macrophage-biomaterial interactions (Rostam et al., 2015; Zaveri et al., 2010a, b). Biomaterial surface chemistry is one factor that impacts cellular responses (Unadkat et al., 2011) as it influences the amount, identity and conformation of protein adsorption on the surface (Sigal et al., 1998), which in turn modulates cell behaviour. For instance, surfaces functionalised with the arginine-glycine-aspartate (RGD) peptide, chitosan, and vitronectin stimulate expression of CD147, CD98, MR, and CD13 (molecules related to macrophage fusion) in monocytes (McNally and Anderson, 2015; Dadsetan et al., 2004; Brodbeck et al., 2002).

Modification of material surface chemistry has been used to change the functional properties and phenotype of different cell types (Murphy et al., 2014; Celiz et al., 2015), including immune cells (Sun et al., 2007; Senaratne et al., 2006). Such strategies would enable the development of materials with cell-instructive properties that could be used for devices such as pacemakers (Taguchi et al., 2014), prosthetic joints (Katti, 2004), intraocular lenses (McCoy et al., 2012), vascular grafts (Xue and Greisler, 2003) and degradable sutures (Cao and Wang, 2009).

In this study, we employed plasma etching, a process used routinely in the mass production of tissue culture ware (Zamora et al., 2003), to develop different surface chemistries using polystyrene as our substrate. We then characterised the phenotype, cytokine profile and functional properties of human monocytes that were cultured on these surfaces for 6 days. Finally, to better understand how these surface chemistries influence monocyte differentiation and macrophage polarisation, we conducted initial characterisation of protein adsorbates on each of the surfaces.

2. Materials and methods

2.1. Materials

All materials were purchased from Sigma-Aldrich unless otherwise stated.

2.2. Surface preparation

Polystyrene samples (2 cm^2) were made by cutting untreated polystyrene (PS) petri dishes (Greiner bio-one Ltd.). Two oxygen plasma etched polystyrene (O_2-PS) surfaces were made by etching untreated PS with O_2 plasma using radio frequency powered equipment described previously (Majani et al., 2010); these were: 1) O_2-PS40 - 40 W, 300 mTorr, 60 s, and 2) O_2-PS8–8W, 300 mTorr, 5 s. Polystyrene tissue culture plates (TCP) (Corning), which have a proprietary treatment, were used as the fourth surface chemistry.

Please cite this article in press as: Rostam, H.M., et al., The impact of surface chemistry modification on macrophage polarisation. Immunobiology (2016), http://dx.doi.org/10.1016/j.imbio.2016.06.010

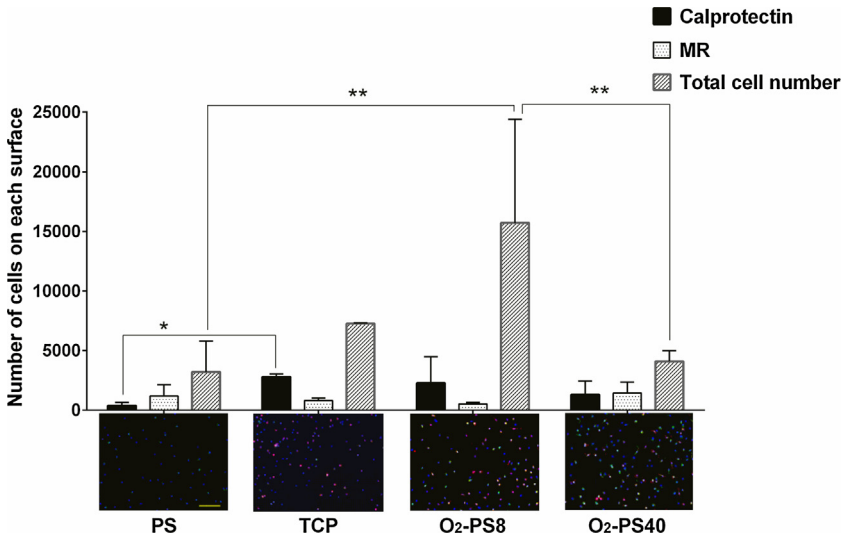

Fig. 2. Monocytes seeded on polystyrene and TCP surfaces for 6 days. The number of adherent cells and calprotectin-MR cell markers expression on PS, O_2-PS and TCP surfaces was measured after 6 days of culture. The graph depicts mean cell number ± SD for n = 6 (O_2-PS40 and PS) and n = 2 (O_2-PS8 and TCP). Cells were stained with rabbit anti-human MR primary antibody and goat anti-rabbit secondary antibody conjugated with Alexa Fluor 488 (green), mouse anti-human 27E10 primary antibody (against calprotectin) and goat anti-mouse secondary antibody conjugated with Rhodamine red-X (red), and DAPI (blue) to visualise the nucleus. Scale bar = 200 μm, all images are at the same magnification (see Supplementary Fig. 1). The number of calprotectin and mannose receptor positive cells on each slide was quantified using CellProfiler. Significance was calculated by one-way ANOVA with Tukey's post test: *, $p \leq 0.05$; **, $p \leq 0.01$.

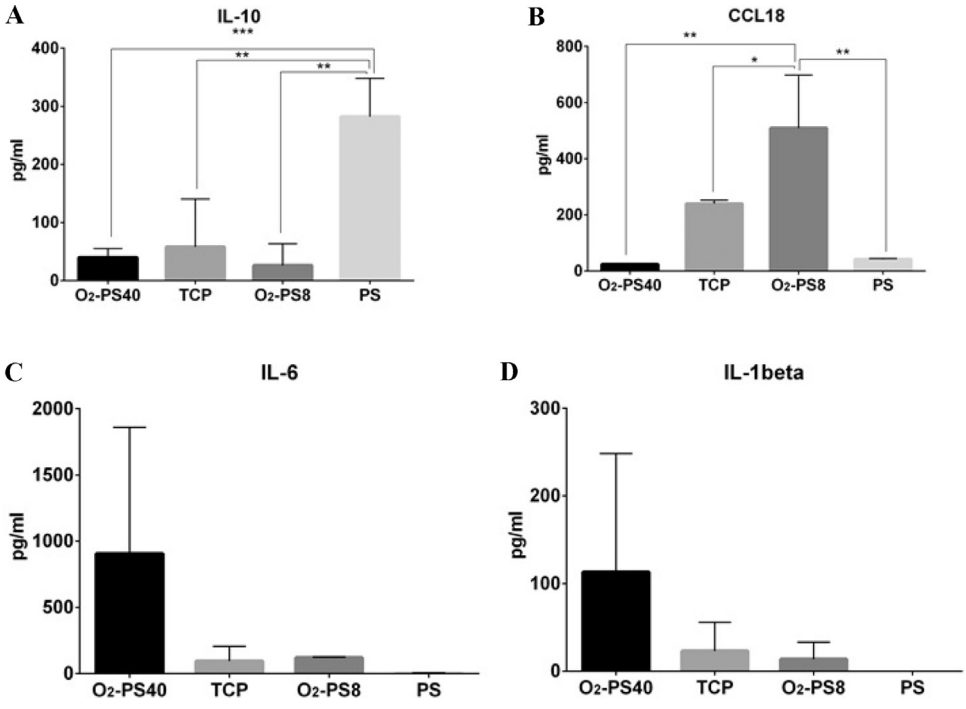

Fig. 3. Cytokine analysis of monocytes seeded on polystyrene and TCP surfaces for 6 days. (A) IL-10, (B) CCL-18, (C) IL-6 and (D) IL-1β. The graphs depict mean cytokine production ± SEM for monocytes seeded on O_2-PS40 and PS (n = 4), O_2-PS8 and TCP (n = 3) surfaces. Significance calculated by one-way ANOVA with Tukey's post test: *, $p \leq 0.05$; **, $p \leq 0.01$; ***, $p \leq 0.001$.

2.3. Water contact angle (WCA) measurement

WCA was measured on an automated DSA100 instrument (Krüss) using pico-litre ultrapure water as previously described (Taylor et al., 2007).

2.4. Atomic force microscopy (AFM)

AFM was carried out on a DimensionTM 3000 AFM equipped with a NanoScope IIIa controller (Veeco Instruments Ltd.) operating in tapping mode in air. The images were processed and analysed with Nanoscope v5.30r2 software and Gwyddion software.

2.5. Time-of-Flight secondary ion mass spectrometry (ToF-SIMS)

An IONTOF GmbH ToF-SIMS IV instrument was used with a Bi^{3+} primary ion source at 25 kV exhibiting a pulsed target current of ~1 pA as previously described (Hook et al., 2013).

Please cite this article in press as: Rostam, H.M., et al., The impact of surface chemistry modification on macrophage polarisation. Immunobiology (2016), http://dx.doi.org/10.1016/j.imbio.2016.06.010

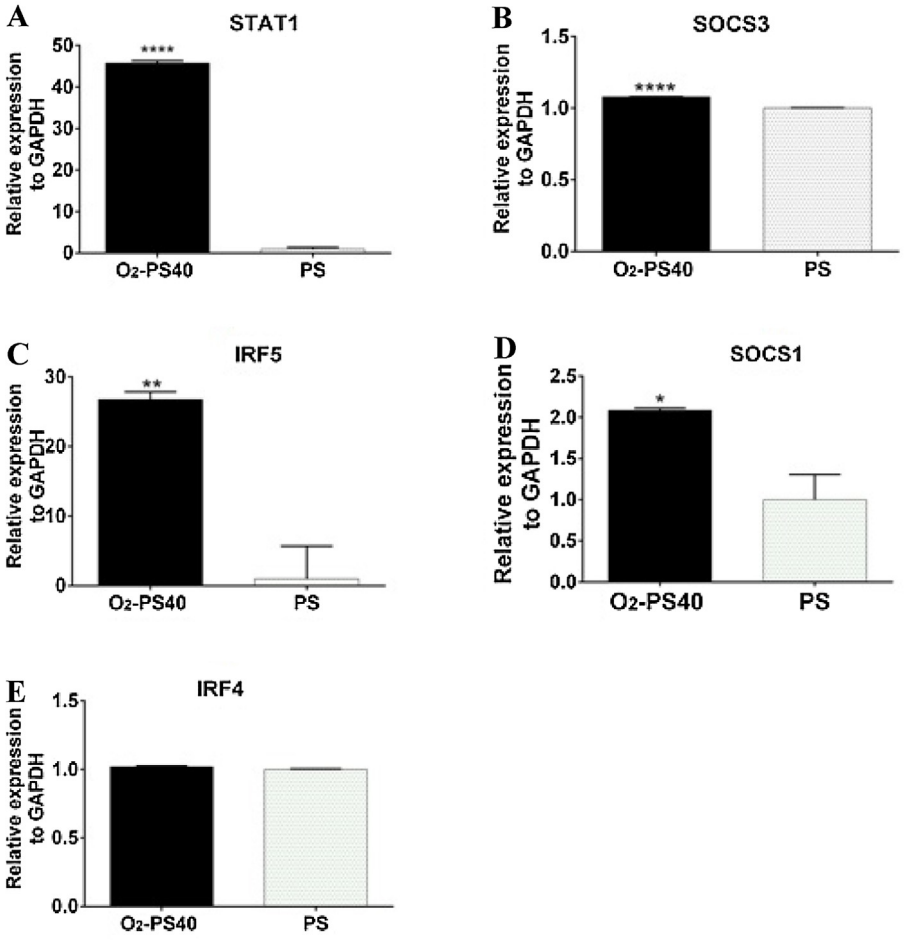

Fig. 4. Comparison of transcription factor mRNA expression in monocytes seeded on un-treated polystyrene (PS) with water contact angle 84.2° and oxygen plasma etched polystyrene (O_2-PS40) with water contact angle 9.8°. qRT-PCR analysis of (A) STAT1, (B) SOCS3, (C) IRF5, (D) SOCS1, (E) IRF4 relative mRNA expression in monocytes on PS and O_2-PS40 macrophages after 6 days of culture. All values are reported relative to the house-keeping gene GAPDH. The graphs depict mean gene expression ± SEM of three different donors (3 technical replicates performed for each donor). Significance calculated by Student's *t*-test: *, $p \leq 0.05$; **, $p \leq 0.01$; ****, $p \leq 0.0001$.

Table 2
Carbon (C), Oxygen (O), and Nitrogen (N) atomic percentage concentration on polystyrene and TCP surfaces before and after incubation with culture medium. Data presented are mean of n = 3.

	Elemental concentration (Atomic%) before incubation with culture medium			Elemental concentration (Atomic%) after incubation with culture medium		
	C	O	N	C	O	N
PS	96.4	2.5	1.1	81.3	11.1	7.5
O_2-PS8	94.0	5.3	0.6	75.9	15.1	9.0
TCP	93.1	6.0	0.8	77.7	13.5	8.8
O_2-PS40	87.1	12.1	0.7	73.1	17.1	9.8

2.6. X-ray photoelectron spectroscopy (XPS)

XPS analysis was carried out using a Theta Probe MKII spectrometer with a micro-focussed monochromated Al Kα source as previously described (Hook et al., 2012).

2.7. Multivariate analysis

Principle component analysis (PCA) was carried out using PLS_Toolbox v5.2 (Eigenvector Research) for Matlab (Mathwords Inc.). Data were mean centred before analysis.

2.8. Monocyte isolation and culture

Buffy coat samples were obtained from healthy volunteers after obtaining written informed consent and approval of the local ethics committee (National Blood Service, Sheffield, United Kingdom). Peripheral blood mononuclear cells (PBMCs) were obtained from buffy coats by Histopaque-1077 density gradient centrifugation. Monocytes were isolated from PBMCs using the MACS magnetic cell separation system (positive selection with CD14 MicroBeads and LS columns, Miltenyi Biotec) as described before (Garcia-Nieto et al., 2010; Harrington et al., 2014). Purified monocytes were suspended in RPMI-1640 medium supplemented with 10% FBS, 2 mM L-glutamine, 100 U/ml penicillin, and 100 μg/ml streptomycin. 3×10^6 monocytes were seeded on each surface and incubated at 37 °C, 5% CO_2 for 6 days.

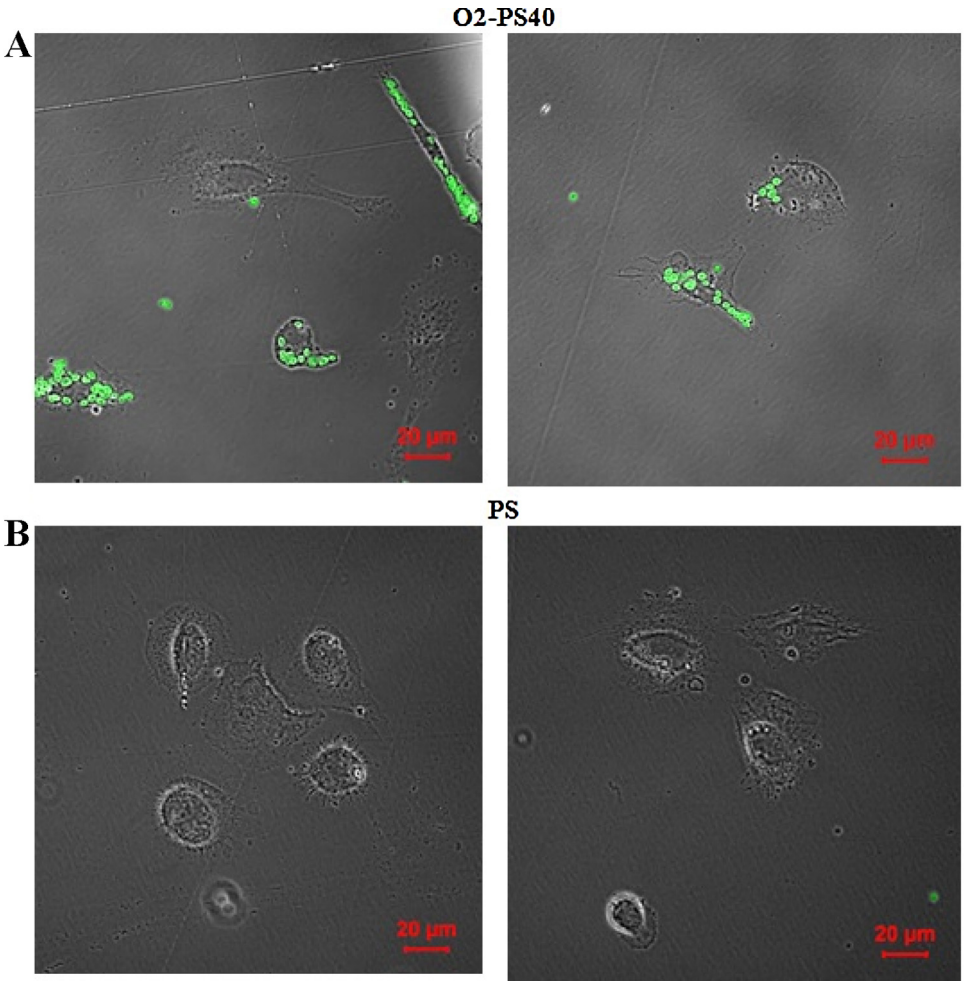

Fig. 5. Phagocytic activity of monocytes cultured on O_2-PS40 and PS surfaces for 6 days. On Day 6 of culture, monocyte-derived macrophages on (A) O_2-PS40 and (B) PS were treated with Alexa Fluor 488-labelled zymosan particles for 30 min at 37 °C, 5% CO_2. Data shown are representative of 3 independent experiments. Scale bar = 20 μm.

2.9. Immunofluorescent staining

Procedure was carried out at room temperature. On day 6, cells were fixed in 4% paraformaldehyde (EMS Diasum) in PBS. Two blocking steps were performed: 1) 3% BSA and 1% glycine (Fisher Scientific) in PBS, 2) 5% goat serum in PBS. Cells were stained with 2 μg/ml mouse anti-human calprotectin antibody (Ab) (Thermo Fisher Scientific) and 1 μg/ml rabbit anti-human MR Ab (Abcam) for 1 h, then stained with 8 μg/ml Rhodamine red X goat anti-mouse IgG(H + L) secondary Ab (Thermo Fisher Scientific) and 8 μg/ml Alexa flour 488 goat anti-rabbit IgG(H + L) secondary Ab (Thermo Fisher Scientific) for 1 h. Cells were counterstained with 250 ng/ml DAPI (Thermo Fisher Scientific), covered with Fluorosave anti-fade medium (Calbiochem) and mounted in Fluoromount medium. Images were taken with an automated fluorescence microscope (IMSTAR) and the data were processed with CellProfiler software v2.1.1.

2.10. Cytokine analysis

IL-6, IL-10, and IL-1β were measured by the FlowCytomix bead-based multiplex system (eBioscience) with a slight modification to the manufacturer's instructions as previously described (Horlock et al., 2007; Wong et al., 2006; Sharquie et al., 2013). Samples were analysed on a Beckman Coulter FC500 flow cytometer. Results were analysed using the eBioscience FlowCytomix Pro 3.0 software.

CCL18 was measured using the human CCL18/PARC DuoSet ELISA kit (R&D Systems) as per the manufacturer's instructions.

2.11. RNA extraction, cDNA conversion, and quantitative real-time PCR (qRT-PCR)

RNA was extracted from cells using RNeasy Plus Minikit (Qiagen) following manufacturer's protocol. cDNA was synthesised from 1 μg of total RNA using the superscript III first-strand synthesis kit (Invitrogen) according to the manufacturer's protocol. Using a LightCycler® 96 machine (Roche), qRT-PCR was performed based on TaqMan and SYBR chemistry. Primers are listed in Table 1. Data were analysed by LightCycler® 96 SW 1.1 software (Roche). Relative expression of genes of interest was calculated by normalising against the house-keeping gene glyceraldehyde 3-phosphate dehydrogenase (GAPDH) based on the relative standard curve method.

2.12. Phagocytosis

Monocytes cultured on surfaces for 6 days were incubated with 25 particles/cell Alexa Fluor 488-conjugated zymosan A (*Saccharomyces cerevisiae*) BioParticles (Thermo Fisher Scientific) at 37 °C, 5% CO_2 for 30 min, then washed 5 times with PBS. Cells were imaged with a Zeiss LSM 880 confocal microscope using a 40× oil objective lens (NA = 1.30), a 488 nm argon laser, and 500–535 nm emission bandwidth. Images were captured using Zen digital imaging software.

Please cite this article in press as: Rostam, H.M., et al., The impact of surface chemistry modification on macrophage polarisation. Immunobiology (2016), http://dx.doi.org/10.1016/j.imbio.2016.06.010

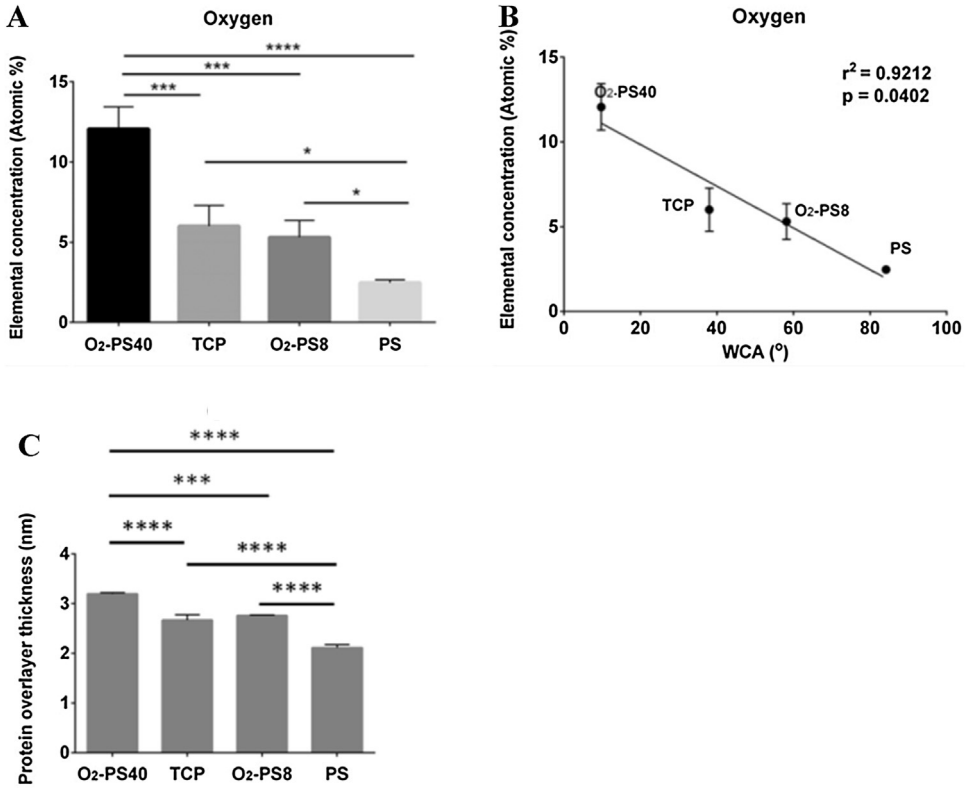

Fig. 6. (A) Oxygen concentration (atomic percent) on polystyrene and TCP surfaces before incubation with cell culture medium (mean ± SD, n = 3). Significance calculated by one-way ANOVA with Tukey's post-test. (B) Pearson correlation of surface oxygen concentration before incubation with medium vs. the WCA of the surfaces (mean ± SD, n = 3). (C) Thickness (nm) of protein overlayer on polystyrene and TCP surfaces. Surfaces were incubated with cell culture medium, following protein overlayer thickness was measured (mean ± SD, n = 3). Significance calculated by one-way ANOVA with Tukey's post-test: *, $p \leq 0.05$; ***, $p \leq 0.001$; ****, $p \leq 0.0001$.

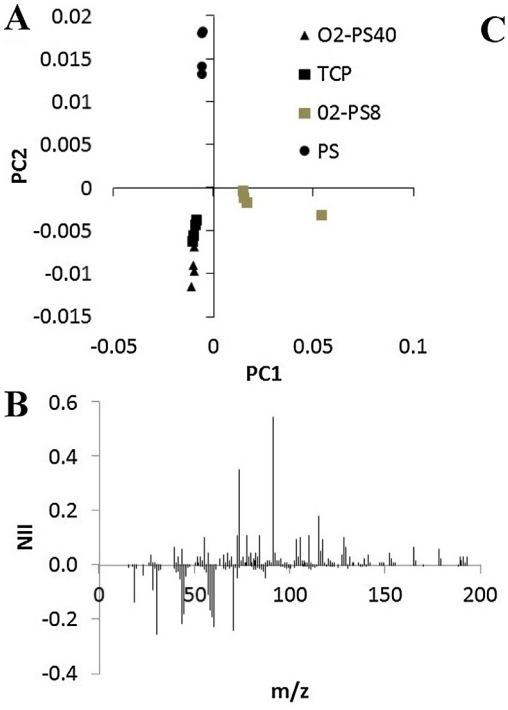

C

Loading	m/z	Assignment	Associated amino acid
0.55	91.0567	$C_7H_7^+$	Tyrosine, phenylalanine
0.35	73.0643	$C_2H_7N_3^+$	
0.18	115.0518	$C_4H_7N_2O_2^+$ $C_9H_7^+$ $C_5H_9SN^+$	
0.11	84.088	$C_5H_{10}N^+$	Lysine
0.11	110.078	$C_5H_{10}N^+$	Histidine
0.11	72.0856	$C_4H_{10}N^+$	Valine
0.11	77.0377	$C_6H_5^+$	
0.11	105.0699	$C_8H_9^+$	
0.10	55.0548	$C_4H_7^+$	
0.10	128.0509	$C_9H_6N^+$ $C_6H_{10}SN^+$ $C_6H_8O_3^+$	
0.10	117.0617	$C_5H_{11}SN^+$ $C_8H_7N^+$ $C_4H_9N_2O_2^+$	
0.10	103.0508	$C_3H_7N_2O_2^+$ $C_8H_7^+$ $C_4H_9SN^+$	Methionine
0.07	165.0663	$C_8H_9N_2O_2^+$ $C_6H_7N_5O^+$	
-0.25	30.0368	CH_4N^+	
-0.24	70.0707	$C_4H_8N^+$	Proline, Arginine
-0.23	60.0554	$CH_6N_3^+$ $C_3H_8O^+$	
-0.22	43.029	$CH_3N_2^+$	
-0.19	59.049	$CH_5N_3^+$ $C_3H_7O^+$	Arginine
-0.18	44.0509	$C_2H_6N^+$	Alanine
-0.17	58.0676	$C_3H_8N^+$	
-0.14	18.0363	H_4N^+	
-0.09	28.0203	CH_2N^+	

Fig. 7. ToF-SIMS analysis of polystyrene and TCP surfaces after incubation with cell culture medium. (A) Scores plot for PCs 1 and 2 using positive ions only. (B) Loading plots for PC2. List of ions with the highest (C) positive or negative loadings for PC2 with corresponding assignments and associated amino acids.

Please cite this article in press as: Rostam, H.M., et al., The impact of surface chemistry modification on macrophage polarisation. Immunobiology (2016), http://dx.doi.org/10.1016/j.imbio.2016.06.010

2.13. Statistical analysis

Statistical analysis was performed on GraphPad Prism 6. Significance was calculated by one-way ANOVA or Student's *t*-test, and correlation was measured by Pearson correlation. P values ≤ 0.05 were considered statistically significant.

3. Results

3.1. Characterisation of polystyrene surface wettability

Polystyrene surface wettability was determined by measuring the WCA of each surface. Untreated PS was the most hydrophobic (WCA = $84^\circ \pm 4^\circ$), followed by O_2-PS8 ($59^\circ \pm 4.7^\circ$), commercial TCP ($38^\circ \pm 9^\circ$), and the most hydrophilic surface, O_2-PS40 ($10^\circ \pm 2^\circ$) (Fig. 1).

3.2. The effect of changes in surface wettability on monocyte attachment and expression of calprotectin and mannose receptor

The number of monocytes adherent to the 4 surfaces after 6 days of incubation was compared. There were significant differences in the number of adherent cells on O_2-PS8 compared to O_2-PS40 ($p = 0.0027$) and PS ($p = 0.0015$) (Fig. 2). Differences between the other conditions were not significant.

Furthermore, the ratio of MR+ to calprotectin+ cells on each surface was measured as an indication of M2 vs. M1 polarisation, respectively. The highest ratio of M2/M1 marker expression was observed in PS followed by O_2-PS40 (Fig. 2). O_2-PS8 showed the lowest M2/M1 ratio (Fig. 2). In terms of total number of cells expressing M1 or M2 markers, the only statistically significant difference was higher number of calprotectin+ cells on TCP compared to PS ($p = 0.0483$).

3.3. A highly hydrophobic surface induces production of IL-10 but not CCL18 by macrophages

Cells on PS produced significantly higher levels of IL-10 compared to O_2-PS40 ($p = 0.0008$), TCP ($p = 0.0050$), and O_2-PS8 ($p = 0.0022$) (Fig. 3A). By comparison, cells on O_2-PS8 produced significantly more CCL18 than cells on any other surface (Fig. 3B). Cells on O_2-PS40 produced the highest levels of IL-6 and IL-1β, with negligible levels produced by cells on PS (Fig. 3C,D).

3.4. A highly hydrophilic surface supports differentiation of monocytes towards pro-inflammatory macrophages

qRT-PCR was used to determine the relative expression of activation state-associated transcription factor mRNA in monocytes differentiated on O_2-PS40 and PS surfaces. Significant increases in the expression of pro-inflammatory transcription factors STAT1 ($p < 0.0001$) and IRF5 ($p = 0.0059$) were seen in monocytes on O_2-PS40 compared to those on PS (Fig. 4A and C). Also, there were significant differences in SOCS1 expression ($p = 0.0239$), but not IRF4 expression ($p = 0.0786$), between monocytes seeded on O_2-PS40 and PS surfaces (Fig. 4D and E). The difference between SOCS3 expression on the two surfaces was negligible, although statistical analysis showed this to be significant (Fig. 4B).

Furthermore, our data shows monocytes differentiated on O_2-PS40 were highly phagocytic as evidenced by the engulfment of fluorescently labelled zymosan particles. Cells differentiated on PS showed negligible phagocytic activity (Fig. 5).

3.5. Characterisation of surface chemistry and protein adsorbate quantification on hydrophobic and hydrophilic surfaces

The oxygen concentration determined by XPS on the surfaces was $2.5 \pm 0.2\%$ on PS, $5.3 \pm 1.1\%$ on O_2-PS8, $6 \pm 1.2\%$ on TCP and $12.0 \pm 1.4\%$ on O_2-PS40 (Table 2). Significant differences in the oxygen concentration of the different surfaces were observed (Fig. 6A). The surface oxygen introduced by plasma etching and proprietary TCP treatment correlated positively with surface hydrophilicity (Fig. 6B, $r^2 = 0.9212$, $p = 0.0402$).

To characterise the surface chemistry of the materials under culture conditions, samples were incubated in culture medium without cells. The nitrogen concentration of each surface was used to quantify the amount of adsorbed protein (Samuel et al., 2001). The protocol used retained strongly adsorbed protein species on the surface but removed weakly adsorbed ones prior to surface analysis

After incubation with the culture medium, significant elemental composition differences were observed for all surfaces (Table 2). The protein overlayer thickness also differed significantly between all the surfaces ($p \leq 0.0001$), except between TCP and O_2-PS8 surfaces ($p = 0.3390$) (Fig. 6C). The following hierarchy was observed for protein overlayer thickness: PS, 2.11 ± 0.06 nm < O_2-PS8, 2.76 ± 0.01 nm < TCP, 2.67 ± 0.11 nm < O_2-PS40, 3.19 ± 0.03 nm. Further, the protein adsorption on these samples showed a strong but non-significant correlation with surface WCA ($r^2 = 0.8727$, $p = 0.0658$) and oxygen atomic percentage before medium treatment ($r^2 = 0.8825$, $p = 0.0606$) (data not shown).

By comparing the observed protein overlayer thickness to the size of the most abundant globular protein in serum, albumin, it can be seen that the protein layer ranges from 2.1 to 3.2 nm monolayers in thickness. Thus, even at the lowest protein coverage, the cells would likely encounter a completely covered polymer surface. Consequently, we sought to gain some insight into the composition of this protein layer through surface mass spectral analysis using ToF-SIMS.

To effectively assess differences in the complex spectra between samples, PCA was used to identify the key variance across the datasets. Plots of PC1 and PC2 for the positively charged ions in the ToF-SIMS data discriminated between all 4 surfaces and replicate measurements clustered together, indicating similarity of the information contained in the spectra (Fig. 7A). All 4 samples were separated from each other using the ions contained in PC2, while PC1 separated O_2-PS8 from the other surfaces (Fig. 7A). For PC2, negative loadings for PC2 were associated with particular amino acids (Fig. 7B)(Samuel et al., 2001), suggesting that a significant contribution in the PS sample had a positive score, whereas the other 3 samples had negative scores, with TCP having a score between the other two samples. The majority of the ions with the highest positive or variance in surface chemistry is associated with differential protein adsorption and/or orientation. Specifically, secondary ions associated with tyrosine and phenylalanine, lysine, histidine, valine, and methionine (Fig. 7C) had positive loadings, indicating a higher intensity of these amino acids on PS samples. For the positive PC2 loadings, it was also notable that there were ions that could have derived from polystyrene, $m/z = 55.0548$ ($C_4H_7^+$); $m/z = 77.0377$ ($C_6H_5^+$); $m/z = 105.0699$ ($C_8H_9^+$), suggesting that there may be areas uncoated by proteins. Ions associated with arginine, alanine, and proline had negative loadings for PC2, indicating that these amino acids were present at a higher intensity on O_2-PS8, TCP, and O_2-PS40 samples. Thus, the surface protein composition was substantially different on the 4 surfaces.

PS and O_2-PS40 surfaces from either ends of the WCA spectrum were selected for topographical characterisation using AFM. Both surfaces had similar roughness, $r_a = 11$ nm (data not shown).

Please cite this article in press as: Rostam, H.M., et al., The impact of surface chemistry modification on macrophage polarisation. Immunobiology (2016), http://dx.doi.org/10.1016/j.imbio.2016.06.010

4. Discussion

In this study we observed monocyte differentiation towards different macrophage phenotypes in response to altered surface chemistry in the absence of exogenous polarising cytokines. Given its widespread use for tissue culture we used polystyrene for surface modification studies. Using O_2 plasma etching we developed 4 surfaces with distinct chemistries that were graded by their surface wettability (measured as WCA). Untreated PS was the most hydrophobic and O_2-PS40 the most hydrophilic. Our data show that the hydrophilic surface O_2-PS40 stimulated monocyte polarisation towards a pro-inflammatory M1-like phenotype while the hydrophobic surface PS had the opposite effect.

The ratio of MR+ (M2-marker (Agrawal, 2012; Mantovani, 2006; Choi et al., 2010)) cells to Calprotectin+ (M1-marker (Bartneck et al., 2010)) cells was ~3 on PS and decreased to ~1 on O_2-PS40 (Fig. 2). This was in line with the cytokine profile of the cells where monocytes cultured on PS secreted significantly higher levels of the anti-inflammatory cytokine IL-10 (Mantovani, 2006) (Fig. 3A). Also, phagocytic activity in PS-cultured cells was negligible compared to O_2-PS40-cultured cells (Fig. 5) (Aderem and Underhill, 1999). It is worth highlighting that the effect of macrophage polarisation on phagocytosis depends upon whether the phagocytosis is Fc-mediated or mediated by a specific pathogen recognition receptor (Martinez and Gordon, 2014; Martinez et al., 2009). While Fc-mediated phagocytosis is thought to be reduced in M1 macrophages, non-Fc-mediated phagocytosis of some pathogens (e.g. Candida albicans) is increased in macrophages with M1 like phenotype (Martinez and Gordon, 2014). This is in line with our observation showing more efficient phagocytosis of zymosan particles by macrophages on O_2-PS40 surfaces which is likely to be mediated through zymosan-specific receptors (Underhill, 2003).

Analysis of transcription factor expression gave a more mixed picture of surface-induced macrophage polarisation. IRF4 was expressed at similar levels in monocytes on both O_2-PS40 and PS surfaces. This corresponds to previous reports of IRF4 gene expression being similar in M-CSF and GM-CSF-induced human macrophages (Krausgruber et al., 2011). Cells on O_2-PS40 expressed highly significant levels of the pro-inflammatory transcription factors STAT1 (Martinez and Gordon, 2014; Sica and Bronte, 2007) and IRF5 (Krausgruber et al., 2011; Weiss et al., 2013) compared to cells grown on PS (Fig. 4). However, O_2-PS40-cultured cells also expressed significantly more SOCS1 (Wilson, 2014; Whyte et al., 2011) than PS-cultured cells. SOCS1 is associated with M2 macrophage activation as it downregulates IFN-γ-driven JAK2/STAT1 and TLR/NF-κB signalling, and promotes arginase 1 expression (Wilson, 2014). Interestingly, Whyte et al. reported that SOCS1 can also inhibit IL-10 secretion (Whyte et al., 2011). This may explain the significant increase in IL-10 production by SOCS1-low cells on PS vs. SOCS1-hi cells and lower IL-10 secretion on O_2-PS40 surfaces (Figs. Fig. 44D and Fig. 33A). Given that the balance of SOCS1 and SOCS3 expression in macrophages affects their activation state (Wilson, 2014), our data suggest that macrophages cultured on polystyrene display a unique phenotype that may be directed towards a more pro-inflammatory or anti-inflammatory state by modifications to surface wettability.

Given the potential impact of surface chemistry on protein absorption, we hypothesised that the impact of different polystyrene surfaces on macrophage polarisation is due to differences in the identity and conformation of proteins adsorbed on these surfaces (Sigal et al., 1998). To test this hypothesis, surface chemistry characterisation of all surfaces was carried out by XPS and ToF-SIMS. The XPS data showed that the greatest total amount of protein was adsorbed on hydrophilic O_2-PS40. Similar results were reported by Grinnell and Feld when they found that fibronectin adhesion to hydrophilic glass was more than to hydrophobic functionalised glass. However, others have reported that fibronectin binds to hydrophobic polystyrene surfaces more than to hydrophilic surfaces (Grinnell and Feld, 1982). Furthermore, ToF-SIMS data confirmed that ions assigned to amino acids arginine, alanine, and proline were more prevalent on O_2-PS40, while ions assigned to tyrosine and phenylalanine, lysine, histidine, valine, and methionine were more prevalent on PS (Fig. 7).

From this surface characterisation we propose that the adsorbed protein, controlled by the polystyrene surface chemistry, influences the macrophage response. An example of known interaction with proteins is macrophage engagement of fibronectin and fibrinogen on implanted biomaterial surfaces through leukocyte β2 integrin receptors (particularly αMβ2 (Mac-1) mediator (Flick et al., 2004; Tang et al., 1996)), which initiates signalling pathways leading to macrophage activation and secretion of inflammatory cytokines such as IL-6, IL-1α, TNF-β (Rostam et al., 2015), and chemotactic factors such as IL-8 and macrophage inflammatory protein 1 beta (MIP-1β) (Jones et al., 2007). In addition to the type of adsorbed proteins, their orientation on a surface can affect the type of macrophage response (Garcia et al., 1999).

5. Conclusions

Our data clearly show that changes in surface chemistry resulting from O_2 introduction by plasma treatment affect protein adsorption on the material. This in turn appears to influence monocyte polarisation towards macrophages with distinct phenotypes. Specifically, hydrophobic PS was shown to suppress expression of M1-associated markers and cytokines while promoting M2-associated markers. On the other hand, highly hydrophilic O_2-PS40 had the opposite effect. Protein overlayer thickness and amino acid profiles were different on hydrophilic and hydrophobic polystyrene, suggesting differences in protein adsorption.

We therefore suggest that changes in the chemistry of material surfaces can be a powerful tool for modulating macrophage phenotype and function without using polarising cytokines. This has clear implications in biomaterial design and function with applications in cell culture and medical device fabrication amongst others.

Conflicts of interest

None.

Acknowledgements

Authors would also like to acknowledge funding from EU FP7 IMMODGEL (Grant No. 602694) and the UK Engineering and Physical Sciences Research Council (EPSRC) (EP/N006615/1). Authors would also like to acknowledge NEXUS Newcastle (http://www.ncl.ac.uk/nexus/) for XPS analysis and Dr David Scurr for help with ToF-SIMS measurements. M.R.A. gratefully acknowledges The Royal Society for provision of the Wolfson Research Merit Award. HR is recipient of a Human Capacity Development Program (HCDP) PhD scholarship (Kurdistan Regional Government).

Appendix A. Supplementary data

Supplementary data associated with this article can be found, in the online version, at http://dx.doi.org/10.1016/j.imbio.2016.06.010.

References

Aderem, A., Underhill, D.M., 1999. Mechanisms of phagocytosis in macrophages. Annu. Rev. Immunol. 17, 593–623.

Agrawal, H., 2012. Macrophage phenotypes correspond with remodeling outcomes of various acellular dermal matrices. Open J. Regener. Med. 01, 51–59.
Anderson, J.M., Rodriguez, A., Chang, D.T., 2008. Foreign body reaction to biomaterials. Semin. Immunol. 20, 86–100.
Baitsch, D., Bock, H.H., Engel, T., Telgmann, R., Muller-Tidow, C., Varga, G., Bot, M., Herz, J., Robenek, H., von Eckardstein, A., Nofer, J.R., 2011. Apolipoprotein E induces antiinflammatory phenotype in macrophages. Arterioscler. Thromb. Vasc. Biol. 31, 1160–1168.
Bartneck, M., Schulte, V.A., Paul, N.E., Diez, M., Lensen, M.C., Zwadlo-Klarwasser, G., 2010. Induction of specific macrophage subtypes by defined micro-patterned structures. Acta Biomater. 6, 3864–3872.
Bartoli, C.R., Godleski, J.J., 2010. Blood flow in the foreign-body capsules surrounding surgically implanted subcutaneous devices. J. Surg. Res. 158, 147–154.
Brodbeck, W.G., Nakayama, Y., Matsuda, T., Colton, E., Ziats, N.P., Anderson, J.M., 2002. Biomaterial surface chemistry dictates adherent monocyte/macrophage cytokine expression in vitro. Cytokine 18, 311–319.
Cao, Y., Wang, B., 2009. Biodegradation of silk biomaterials. Int. J. Mol. Sci. 10, 1514–1524.
Celiz, A.D., Smith, J.G.W., Patel, A.K., Hook, A.L., Rajamohan, D., George, V.T., Flatt, L., Patel, M.J., Epa, V.C., Singh, T., Langer, R., Anderson, D.G., Allen, N.D., Hay, D.C., Winkler, D.A., Barrett, D.A., Davies, M.C., Young, L.E., Denning, C., Alexander, M.R., 2015. Discovery of a novel polymer for human pluripotent stem cell expansion and multilineage differentiation. Adv. Mater. 27, 4006–4012.
Choi, K.M., Kashyap, P.C., Dutta, N., Stoltz, G.J., Ordog, T., Donohue, T.S., Bauer, A.J., Linden, D.R., Szurszewski, J.H., Gibbons, S.J., Farrugia, G., 2010. CD206-positive M2 macrophages that express heme oxygenase-1 protect against diabetic gastroparesis in mice. Gastroenterology 138, 2399-U2261.
Dadsetan, M., Jones, J.A., Hiltner, A., Anderson, J.M., 2004. Surface chemistry mediates adhesive structure, cytoskeletal organization, and fusion of macrophages. J. Biomed. Mater. Res. A 71, 439–448.
Edin, S., Wikberg, M.L., Dahlin, A.M., Rutegard, J., Oberg, A., Oldenborg, P.A., Palmqvist, R., 2012. The distribution of macrophages with a M1 or M2 phenotype in relation to prognosis and the molecular characteristics of colorectal cancer. PLoS One 7, e47045.
Flick, M.J., Du, X.L., Degen, J.L., 2004. Fibrin(ogen)alpha(M)beta(2) interactions regulate leukocyte function and innate immunity in vivo. Exp. Biol. Med. 229, 1105–1110.
Garcia, A.J., Vega, M.D., Boettiger, D., 1999. Modulation of cell proliferation and differentiation through substrate-dependent changes in fibronectin conformation. Mol. Biol. Cell 10, 785–798.
Garcia, S., Krausz, S., Ambarus, C.A., Fernandez, B.M., Hartkamp, L.M., van Es, I.E., Hamann, J., Baeten, D.L., Tak, P.P., Reedquist, K.A., 2014. Tie2 signaling cooperates with TNF to promote the pro-Inflammatory activation of human macrophages independently of macrophage functional phenotype. PLoS One 9.
Garcia-Nieto, S., Johal, R.K., Shakesheff, K.M., Emara, M., Royer, P.J., Chau, D.Y.S., Shakib, F., Ghaemmaghami, A.M., 2010. Laminin and fibronectin treatment leads to generation of dendritic cells with superior endocytic capacity. PLoS One 5.
Grinnell, F., Feld, M.K., 1982. Fibronectin adsorption on hydrophilic and hydrophobic surfaces detected by antibody binding and analyzed during cell adhesion in serum-containing medium. J. Biol. Chem. 257, 4888–4893.
Hamilton, J.A., 2002. GM-CSF in inflammation and autoimmunity. Trends Immunol. 23, 403–408.
Hamilton, J.A., 2008. Colony-stimulating factors in inflammation and autoimmunity. Nat. Rev. Immunol. 8, 533–544.
Hao, N.B., Lu, M.H., Fan, Y.H., Cao, Y.L., Zhang, Z.R., Yang, S.M., 2012. Macrophages in tumor microenvironments and the progression of tumors. Clin. Dev. Immunol. 2012, 948098.
Harrington, H., Cato, P., Salazar, F., Wilkinson, M., Knox, A., Haycock, J.W., Rose, F., Aylott, J.W., Ghaemmaghami, A.M., 2014. Immunocompetent 3D model of human upper airway for disease modeling and in vitro drug evaluation. Mol. Pharmaceutics 11, 2082–2091.
Higgins, D.M., Basaraba, R.J., Hohnbaum, A.C., Lee, E.J., Grainger, D.W., Gonzalez-Juarrero, M., 2009. Localized immunosuppressive environment in the foreign body response to implanted biomaterials. Am. J. Pathol. 175, 161–170.
Hofkens, W., Storm, G., van den Berg, W., van Lent, P., 2011. Inhibition of M1 macrophage activation in favour of M2 differentiation by liposomal targeting of glucocorticoids to the synovial lining during experimental arthritis. Ann. Rheum. Dis. 70, A40–A40.
Hook, A.L., Chang, C.Y., Yang, J., Scurr, D.J., Langer, R., Anderson, D.G., Atkinson, S., Williams, P., Davies, M.C., Alexander, M.R., 2012. Polymer microarrays for high throughput discovery of biomaterials. JoVE–J. Vis. Exp.
Hook, A.L., Scurr, D.J., Anderson, D.G., Langer, R., Williams, P., Davies, M., Alexander, M., 2013. High throughput discovery of thermo-responsive materials using water contact angle measurements and time-of-flight secondary ion mass spectrometry. Surf. Interface Anal. 45, 181–184.
Horlock, C., Shakib, F., Mahdavi, J., Jones, N.S., Sewell, H.F., Ghaemmaghami, A.M., 2007. Analysis of proteomic profiles and functional properties of human peripheral blood myeloid dendritic cells, monocyte-derived dendritic cells and the dendritic cell-like KG-1 cells reveals distinct characteristics. Genome Biol. 8, R30.
Jones, J.A., Chang, D.T., Meyerson, H., Colton, E., Kwon, I.K., Matsuda, T., Anderson, J.M., 2007. Proteomic analysis and quantification of cytokines and chemokines from biomaterial surface-adherent macrophages and foreign body giant cells. J. Biomed. Mater. Res. A 83, 585–596.
Katti, K.S., 2004. Biomaterials in total joint replacement. Colloids Surf. B Biointerfaces 39, 133–142.
Krausgruber, T., Blazek, K., Smallie, T., Alzabin, S., Lockstone, H., Sahgal, N., Hussell, T., Feldmann, M., Udalova, I.A., 2011. IRF5 promotes inflammatory macrophage polarization and TH1-TH17 responses. Nat. Immunol. 12, 231–238.
Majani, R., Zelzer, M., Gadegaard, N., Rose, F.R., Alexander, M.R., 2010. Preparation of Caco-2 cell sheets using plasma polymerised acrylic acid as a weak boundary layer. Biomaterials 31, 6764–6771.
Mantovani, A., 2006. Macrophage diversity and polarization: in vivo veritas. Blood 108, 408–409.
Mantovani, A., Sica, A., Sozzani, S., Allavena, P., Vecchi, A., Locati, M., 2004. The chemokine system in diverse forms of macrophage activation and polarization. Trends Immunol. 25, 677–686.
Martinez, F.O., Gordon, S., 2014. The M1 and M2 paradigm of macrophage activation: time for reassessment. F1000Prime Rep. 6, 13.
Martinez, F.O., Helming, L., Gordon, S., 2009. Alternative activation of macrophages: an immunologic functional perspective. Annu. Rev. Immunol. 27, 451–483.
McCoy, C.P., Craig, R.A., McGlinchey, S.M., Carson, L., Jones, D.S., Gorman, S.P., 2012. Surface localisation of photosensitisers on intraocular lens biomaterials for prevention of infectious endophthalmitis and retinal protection. Biomaterials 33, 7952–7958.
McNally, A.K., Anderson, J.M., 2015. Phenotypic expression in human monocyte-derived interleukin-4-induced foreign body giant cells and macrophages in vitro: dependence on material surface properties. J. Biomed. Mater. Res. A 103, 1380–1390.
Mills, C.D., Kincaid, K., Alt, J.M., Heilman, M.J., Hill, A.M., 2000. M-1/M-2 macrophages and the Th1/Th2 paradigm. J. Immunol. 164, 6166–6173.
Morais, J.M., Papadimitrakopoulos, F., Burgess, D.J., 2010. Biomaterials/tissue interactions: possible solutions to overcome foreign body response. AAPS J. 12, 188–196.
Murphy, W.L., McDevitt, T.C., Engler, A.J., 2014. Materials as stem cell regulators. Nat. Mater. 13, 547–557.
Murray, P.J., Wynn, T.A., 2011. Protective and pathogenic functions of macrophage subsets. Nat. Rev. Immunol. 11, 723–737.
Rostam, H.M., Singh, S., Vrana, N.E., Alexander, M.R., Ghaemmaghami, A.M., 2015. Impact of surface chemistry and topography on the function of antigen presenting cells. Biomater. Sci. 3, 424–441.
Samuel, N.T., Wagner, M.S., Dornfeld, K.D., Castner, D.G., 2001. Analysis of poly(amino acids) by static time-of-flight secondary ion mass spectrometry (TOF-SIMS). Surf. Sci. Spectra 8, 163–184.
Senaratne, W., Sengupta, P., Jakubek, V., Holowka, D., Ober, C.K., Baird, B., 2006. Functionalized surface arrays for spatial targeting of immune cell signaling. J. Am. Chem. Soc. 128, 5594–5595.
Sharquie, I.K., Al-Ghouleh, A., Fitton, P., Clark, M.R., Armour, K.L., Sewell, H.F., Shakib, F., Ghaemmaghami, A.M., 2013. An investigation into IgE-facilitated allergen recognition and presentation by human dendritic cells. BMC Immunol. 14.
Shen, M., Garcia, I., Maier, R.V., Horbett, T.A., 2004. Effects of adsorbed proteins and surface chemistry on foreign body giant cell formation, tumor necrosis factor alpha release and procoagulant activity of monocytes. J. Biomed. Mater. Res. A 70, 533–541.
Sica, A., Bronte, V., 2007. Altered macrophage differentiation and immune dysfunction in tumor development. J. Clin. Invest. 117, 1155–1166.
Sica, A., Mantovani, A., 2012. Macrophage plasticity and polarization: in vivo veritas. J. Clin. Invest. 122, 787–795.
Sigal, G.B., Mrksich, M., Whitesides, G.M., 1998. Effect of surface wettability on the adsorption of proteins and detergents. J. Am. Chem. Soc. 120, 3464–3473.
Solheim, E., Sudmann, B., Bang, G., Sudmann, E., 2000. Biocompatibility and effect on osteogenesis of poly(ortho ester) compared to poly(DL-lactic acid). J. Biomed. Mater. Res. 49, 257–263.
Sun, T., Han, D., Riehemann, K., Chi, L.F., Fuchs, H., 2007. Stereospecific interaction between immune cells and chiral surfaces (vol 129, pg 1496, 2007). J. Am. Chem. Soc. 129, 4853–4853.
Sutterwala, F.S., Noel, G.J., Clynes, R., Mosser, D.M., 1997. Selective suppression of interleukin-12 induction after macrophage receptor ligation. J. Exp. Med. 185, 1977–1985.
Taguchi, T., Maeba, S., Sueda, T., 2014. Prevention of pacemaker-associated contact dermatitis by polytetrafluoroethylene sheet and conduit coating of the pacemaker system. J. Artif. Organs 17, 285–287.
Tang, L., Ugarova, T.P., Plow, E.F., Eaton, J.W., 1996. Molecular determinants of acute inflammatory responses to biomaterials. J. Clin. Invest. 97, 1329–1334.
Taylor, M., Urquhart, A.J., Zelzer, M., Davies, M.C., Alexander, M.R., 2007. Picoliter water contact angle measurement on polymers. Langmuir 23, 6875–6878.
Unadkat, H.V., Hulsman, M., Cornelissen, K., Papenburg, B.J., Truckenmuller, R.K., Carpenter, A.E., Wessling, M., Post, G.F., Uetz, M., Reinders, M.J., Stamatialis, D., van Blitterswijk, C.A., de Boer, J., 2011. An algorithm-based topographical biomaterials library to instruct cell fate. Proc. Natl. Acad. Sci. U. S. A. 108, 16565–16570.
Underhill, D.M., 2003. Macrophage recognition of zymosan particles. J. Endotoxin Res. 9, 176–180.
Verreck, F.A.W., de Boer, T., Langenberg, D.M.L., Hoeve, M.A., Kramer, M., Vaisberg, E., Kastelein, R., Kolk, A., de Waal-Malefyt, R., Ottenhoff, T.H.M., 2004. Human IL-23-producing type 1 macrophages promote but IL-10-producing type 2, macrophages subvert, immunity to (myco)bacteria. Proc. Natl. Acad. Sci. U.S.A. 101, 4560–4565.

Please cite this article in press as: Rostam, H.M., et al., The impact of surface chemistry modification on macrophage polarisation. Immunobiology (2016), http://dx.doi.org/10.1016/j.imbio.2016.06.010

Weiss, M., Blazek, K., Byrne, A.J., Perocheau, D.P., Udalova, I.A., 2013. IRF5 is a specific marker of inflammatory macrophages in vivo. Mediators Inflammation 2013, 245804.
Whyte, C.S., Bishop, E.T., Ruckerl, D., Gaspar-Pereira, S., Barker, R.N., Allen, J.E., Rees, A.J., Wilson, H.M., 2011. Suppressor of cytokine signaling (SOCS)1 is a key determinant of differential macrophage activation and function. J. Leukocyte Biol. 90, 845–854.
Willenborg, S., Lucas, T., van Loo, G., Knipper, J.A., Krieg, T., Haase, I., Brachvogel, B., Hammerschmidt, M., Nagy, A., Ferrara, N., Pasparakis, M., Eming, S.A., 2012. CCR2 recruits an inflammatory macrophage subpopulation critical for angiogenesis in tissue repair. Blood 120, 613–625.
Wilson, H.M., 2014. SOCS proteins in macrophage polarization and function. Front. Immunol. 5, 357.
Wong, C.K., Li, M.L., Wang, C.B., Ip, W.K., Tian, Y.P., Lam, C.W., 2006. House dust mite allergen Der p 1 elevates the release of inflammatory cytokines and expression of adhesion molecules in co-culture of human eosinophils and bronchial epithelial cells. Int. Immunol. 18, 1327–1335.
Xia, Z., Triffitt, J.T., 2006. A review on macrophage responses to biomaterials. Biomed. Mater. 1, R1–R9.
Xue, L., Greisler, H.P., 2003. Biomaterials in the development and future of vascular grafts. J. Vasc. Surg. 37, 472–480.
P.O., Zamora, S., Osaki, M., Chen, 2003. Plasma-deposited coatings, devices and methods, Google Patents.
Zaveri, T.D., Dolgova, N.V., Chu, B.H., Lee, J.Y., Wong, J.E., Lele, T.P., Ren, F., Keselowsky, B.G., 2010a. Contributions of surface topography and cytotoxicity to the macrophage response to zinc oxide nanorods. Biomaterials 31, 2999–3007.
Zaveri, T.D., Dolgova, N.V., Chu, B.H., Lee, J., Wong, J., Lele, T.P., Ren, F., Keselowsky, B.G., 2010b. Contributions of surface topography and cytotoxicity to the macrophage response to zinc oxide nanorods. Biomaterials 31, 2999–3007.

Please cite this article in press as: Rostam, H.M., et al., The impact of surface chemistry modification on macrophage polarisation. Immunobiology (2016), http://dx.doi.org/10.1016/j.imbio.2016.06.010